This is a repository copy of *Metastable States of ^{92,94}Se:Identification of an Oblate K Isomer of ^{94}Se and the Ground-State Shape Transition between N=58 and 60*.

Metastable States of ^{92,94}Se: Identification of an Oblate K Isomer of ^{94}Se and the Ground-State Shape Transition between $N = 58$ and 60

C. Lizarazo,[1,2] P.-A. Söderström[1,3,4,*] V. Werner,[1] N. Pietralla,[1] P. M. Walker,[5] G. X. Dong,[6] F. R. Xu,[7] T. R. Rodríguez,[8] F. Browne,[9] P. Doornenbal,[3] S. Nishimura,[3] C. R. Niţă,[10] A. Obertelli,[1,3,11] T. Ando,[3,12] T. Arici,[2] G. Authelet,[11] H. Baba,[3] A. Blazhev,[13] A. M. Bruce,[9] D. Calvet,[11] R. J. Caroll,[5] F. Château,[11] S. Chen,[3,7] L. X. Chung,[14] A. Corsi,[11] M. L. Cortés,[1,2,3] A. Delbart,[11] M. Dewald,[13] B. Ding,[15] F. Flavigny,[16] S. Franchoo,[16] J. Gerl,[2] J.-M. Gheller,[11] A. Giganon,[11] A. Gillibert,[11] M. Górska,[2] A. Gottardo,[16] I. Kojouharov,[2] N. Kurz,[2] V. Lapoux,[11] J. Lee,[17] M. Lettmann,[1] B. D. Linh,[14] J. J. Liu,[17] Z. Liu,[15,18] S. Momiyama,[3,12] K. Moschner,[13] T. Motobayashi,[3] S. Nagamine,[12] N. Nakatsuka,[19] M. Niikura,[12] C. Nobs,[9] L. Olivier,[16] Z. Patel,[5] N. Paul,[11,3] Zs. Podolyák,[5] J.-Y. Roussé,[11] M. Rudigier,[5] T. Y. Saito,[12] H. Sakurai,[3,12] C. Santamaria,[11] H. Schaffner,[2] C. Shand,[5] I. Stefan,[16] D. Steppenbeck,[3] R. Taniuchi,[3,12] T. Uesaka,[3] V. Vaquero,[20] K. Wimmer,[12] and Z. Xu[17]

[1]*Institut für Kernphysik, Technische Universität Darmstadt, 64289 Darmstadt, Germany*
[2]*GSI Helmholtzzentrum für Schwerionenforschung GmbH, 64291 Darmstadt, Germany*
[3]*RIKEN Nishina Center, 2-1 Hirosawa, Wako, Saitama 351-0198, Japan*
[4]*Extreme Light Infrastructure-Nuclear Physics (ELI-NP)/Horia Hulubei National Institute for Physics and Nuclear Engineering (IFIN-HH), Strada Reactorului 30, 077125 Bucharest-Măgurele, Romania*
[5]*Department of Physics, University of Surrey, Guildford GU2 7XH, United Kingdom*
[6]*School of Science, Huzhou University, Huzhou 313000, China*
[7]*State Key Laboratory of Nuclear Physics and Technology, Peking University, Beijing 100871, People's Republic of China*
[8]*Departamento de Física Teórica, Universidad Autónoma de Madrid, 28049, Spain*
[9]*School of Computing Engineering and Mathematics, University of Brighton, Brighton BN2 4GJ, United Kingdom*
[10]*Department of Nuclear Physics (DFN)/Horia Hulubei National Institute for Physics and Nuclear Engineering (IFIN-HH), Strada Reactorului 30, 077125 Bucharest-Măgurele, Romania*
[11]*IRFU, CEA, Université Paris—Saclay, F-91191 Gif-sur-Yvette, France*
[12]*Department of Physics, University of Tokyo, 7-3-1 Hongo, Bunkyo, Tokyo 113-0033, Japan*
[13]*Institut für Kernphysik, Universität zu Köln, D-50937 Cologne, Germany*
[14]*Institute for Nuclear Science and Technology, VINATOM, P.O. Box 5T-160, Nghia Do, Hanoi, Vietnam*
[15]*Institute of Modern Physics, Chinese Academy of Sciences, Lanzhou 730000, People's Republic of China*
[16]*Institut de Physique Nucléaire Orsay, IN2P3-CNRS, 91406 Orsay Cedex, France*
[17]*Department of Physics, The University of Hong Kong, Pokfulam, Hong Kong*
[18]*School of Nuclear Science and Technology, University of Chinese Academy of Sciences, Beijing 100049, People's Republic of China*
[19]*Department of Physics, Faculty of Science, Kyoto University, Kyoto 606-8502, Japan*
[20]*Instituto de Estructura de la Materia, CSIC, 28006 Madrid, Spain*

Here we present new information on the shape evolution of the very neutron-rich ^{92,94}Se nuclei from an isomer-decay spectroscopy experiment at the Radioactive Isotope Beam Factory at RIKEN. High-resolution germanium detectors were used to identify delayed γ rays emitted following the decay of their isomers. New transitions are reported extending the previously known level schemes. The isomeric levels are interpreted as originating from high-K quasineutron states with an oblate deformation of $\beta \sim 0.25$, with the high-K state in ^{94}Se being metastable and K hindered. Following this, ^{94}Se is the lowest-mass neutron-rich nucleus known to date with such a substantial K hindrance. Furthermore, it is the first observation of an oblate K isomer in a deformed nucleus. This opens up the possibility for a new region of K isomers at low Z and at oblate deformation, involving the same neutron orbitals as the prolate orbitals within the classic $Z \sim 72$ deformed hafnium region. From an interpretation of the level scheme guided by theoretical calculations, an oblate deformation is also suggested for the ^{94}Se$_{60}$ ground-state band.

Neutron-rich nuclei very far from the region of stability, and the nuclear dynamics associated with systems with a large N/Z ratio, have gained considerable interest in recent years. One particular aspect of these systems is the understanding of the nuclear shape at low excitation energies, a property determined by the underlying interplay between the collective and single-particle degrees of freedom in a nucleus. Experimental signatures of the

deformation of even-even nuclei are often found in the $E(2_1^+)$ excitation energy, the $R_{4/2} = E(4_1^+)/E(2_1^+)$ ratio, and the $B(E2; 2_1^+ \rightarrow 0_1^+)$ reduced transition probability, while the sign of the quadrupole moment gives information about the prolate or oblate character of the deformation [1]. The systematic measurement of these observables along an isotopic chain reveals information about shape evolution, like the known spherical-to-prolate ground-state shape transition from $^{98}Zr_{58}$ to $^{100}Zr_{60}$ [2–6].

Nevertheless, for the majority of nuclei, the simplistic interpretation of the shape is not possible, as these observables take intermediate values between the benchmark limits, implying softness of the nuclear shapes or mixing of nuclear wave function components with different deformations. In the case for the neutron-rich $^{86-94}Se_{52-60}$ isotopes, the available data so far unveil a rather smooth systematic behavior beyond the $N = 50$ shell closure [7–10]. The excitation energies of the first $J^\pi = 2^+$ states, $E(2_1^+)$, decrease gradually from 704 ($^{86}Se_{52}$) to 470 keV ($^{94}Se_{60}$), which is one possible indicator of an increase of collectivity with increasing neutron number. Up to $^{92}Se_{58}$, it is observed that $E(2_2^+)$ is below $E(4_1^+)$ and decays with an intense branch to the 2_1^+ state, suggesting the influence of nonaxial γ deformations [1,11,12], such as recently reported for the neighboring nucleus ^{86}Ge [13]. The $R_{4/2}$ values remain around 2.4, typical for the transitional regime between the spherical vibrator (2.0) and the axial rigid rotor (3.33) limits.

For $^{90-94}Se_{56-60}$, recent beyond-mean-field theories have predicted a nuclear potential with coexisting prolate and oblate minima, however, with different detailed shape evolution scenarios for the ground-state. The five-dimensional collective Hamiltonian (5DCH) approximation [14] suggests that these isotopes remain γ-soft deformed, with the axial deformation β increasing with the neutron number N, while the full symmetry-conserving configuration-mixing (SCCM) [15] based on the same interaction and the Hartree-Fock-Bogoliubov (HFB)+ Interacting Boson Model [16] method propose a prolate-to-oblate transition from ^{90}Se to ^{94}Se with pronounced prolate and oblate minima, closest in energy in ^{92}Se, but a certain degree of γ softness. The SCCM and 5DCH calculations show a qualitative agreement with the excitation energies of a few low-lying levels known so far, but the data favor neither.

A special type of excitation can be observed in deformed atomic nuclei, whereby two quasiparticle (2-QP) states are formed by the breaking of pairs of nucleons close to the Fermi level. For $\beta \neq 0$ the single-particle levels rearrange as described by the Nilsson model [17]. A 2-QP state can only couple to an angular momentum $J^\pi = |K_1 \pm K_2|^{\pi_1\pi_2}$, with π_i and K_i as the parity and angular momentum projection of the orbitals occupied by the quasiparticles onto the nuclear symmetry axis. The appearance of such a state is a clear fingerprint of the deformation. J^π is determined exclusively

by levels near the Fermi surface, which are fixed by the sign and magnitude of β. Furthermore, these states become metastable when the transition is K forbidden [18–22], i.e., $\Delta K > \lambda$, with ΔK as the difference in K between the levels involved and λ as the transition multipolarity.

Oblate 2-QP states are very uncommon in the nuclear chart, with no other metastable case reported besides the 11^- K isomer of spherical $^{188-196}Pb$ [23,24] and no confirmed observation in a deformed nucleus. Metastable 2-QP states with high-K values occur more frequently for nuclei with the (proton or neutron) Fermi level in the upper half of a major shell, where the density of high-K levels in the Nilsson diagrams is high, in particular for prolate deformations ($\beta \geq 0$) [18]. Abundant examples can be found in the well-deformed $A \approx 170–180$, $Z \sim 72$ region [25]. Our current observations reflect the counterpart characteristic of the Nilsson diagrams: When the Fermi level is near the middle of a major shell, high-K 2-QP states can also be formed at oblate deformations due to the downsloping Nilsson orbitals from higher-lying high-j configurations. This opens up the possibility for a new region of K isomers at low Z and at oblate deformation for exotic nuclei, involving the same orbitals as within the prolate deformed $Z \sim 72$ region.

In the present Letter, we report on the observation of such states for $^{92,94}Se$ through new data obtained employing isomer-decay spectroscopy, as well as the impact of their decay pattern on the discussion of shape evolution at $N = 60$.

The experiment was performed at the Radioactive Isotope Beam Factory at RIKEN. A radioactive cocktail beam of exotic nuclei centered around $^{95}_{35}Br_{60}$ was delivered by the BigRIPS fragment separator [26], tuned to select the desired subproducts of the in-flight fission of a 345 AMeV ^{238}U primary beam colliding at $\sim$30 pnA intensity with a 3-mm-thick ^9Be target. The secondary beam impinged on the 99(1)-mm-thick liquid-hydrogen target of the MagIc Numbers Off Stability (MINOS) device [27] placed at the focal plane F8. The deexcitation of the products following nucleon-knockout reactions was studied via in-beam γ-ray spectroscopy using the NaI(Tl) detector array for low intensity radiation (DALI2) detector array [28], for details see Refs. [10,13,29–33]. The selenium nuclei discussed here were produced both at the production and the secondary targets.

Behind F8 the reaction products were transported through the ZeroDegree forward spectrometer [26] to identify the nuclei on an event-by-event basis via the TOF-$B\rho$-ΔE measurement to deduce the mass-to-charge ratio (A/Q) and atomic number (Z). We measured the time of flight (TOF) between the F8 and F11 focal planes, $B\rho$ between F9 and F11, and ΔE in the ionization chambers at F11.

The Advanced Implantation Detector Array (AIDA) [34], placed at the end of the ZeroDegree spectrometer, was used to stop and implant the nuclei in the center of the

γ-ray detector system, the Euroball-RIKEN Cluster Array (EURICA) [35], consisting of 84 high-purity Ge crystals arranged in sevenfold clusters pointing toward the center of the stopper at a distance of ~ 22 cm. A $100 - \mu s$ time window was opened when an ion passed through the plastic scintillator located ~ 1 m upstream of the implantation point and was used to record the energy (E_γ) and time (t_γ) of the γ rays. The detection time t_γ was measured relative to the plastic scintillator, with a digital resolution of 25 ns. The relative γ-ray efficiency was measured with and without add back and was consistent with the commissioning values [35]. The average times of flight from the production and from the secondary targets to the stopper were ~ 650 and ~ 380 ns, respectively.

The energy spectra of delayed γ rays correlated with ^{92,94}Se are shown in Fig. 1. For ^{92}Se, γ rays detected within $0.19 \leq t_\gamma \leq 70$ μs relative to implantation were used. This condition suppressed the intense radiation from the ion implantation and reduced the accumulation of environmental background
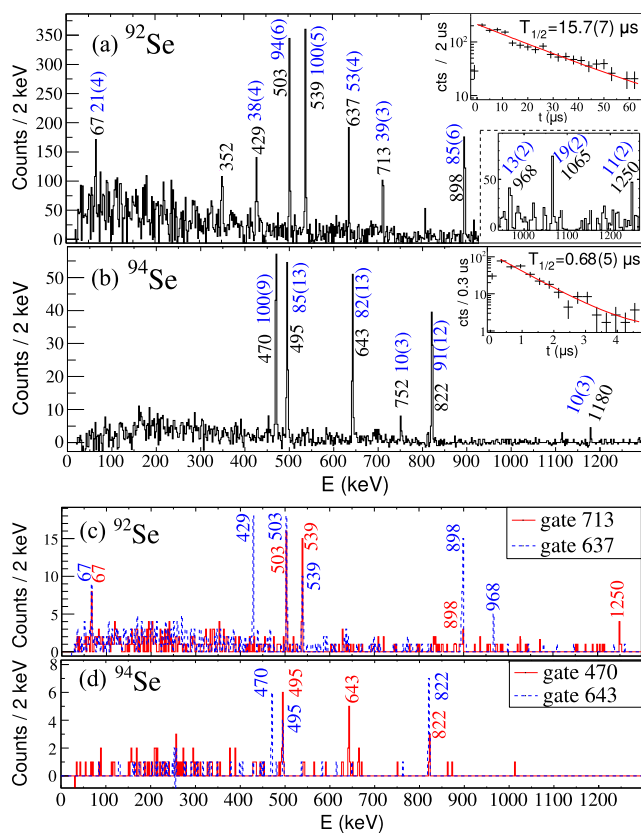

FIG. 1. Delayed γ rays correlated with (a) ^{92}Se and (b) ^{94}Se. The energy in keV (black) and efficiency-corrected intensity relative to the strongest transition (blue) are shown next to the corresponding peaks. The histogram of the total time distribution, used to measure the isomeric state half-life, is displayed in the insets in the top-right corners. For better visibility, the inset at the bottom right of (a) displays the enlarged energy spectrum between 945 and 1260 keV. Examples of $\gamma\gamma$-coincidence energy spectra gated on transitions of (c) ^{92}Se and (d) ^{94}Se are shown.

while preserving the events from isomeric γ rays. A spectrum of events with $t_\gamma \geq 70$ μs was scaled and subtracted to further reduce the environmental background component. All transitions so far reported [10,36] for this nucleus were observed, in addition to new transitions with energies of 66.8(3), 351.9(3), and 1250.2(3) keV. The half-lives inferred from the time distribution of the individual transitions were consistent with each other within statistical uncertainties, indicating the decay of one common isomeric state. The weighted average of the isomeric half-life was $T_{1/2} = 15.7(7)\mu s$, determined using an exponential decay curve plus a constant baseline. The proposed decay scheme following the isomeric decay is shown in Fig. 2 and is similar to recent observations in ^{94}Kr [37]. It was deduced from energy-sum checks, $\gamma\gamma$ coincidences, and sums of efficiency-corrected intensities [38]. The previously observed 898- and 503-keV transitions in ^{92}Se were placed for the first time. The 352-keV transition is inferred despite a strong 351-keV background peak, given an intensity difference of $I_{898} - I_{1065} - I_{637} \approx 13(6)\%$, and a weak coincidence of the 713- and 898-keV transitions. The spins and parities were assigned based on the decay patterns. The internal conversion coefficient of the 67-keV transition was obtained as the average between $\alpha_1 = I_{503}/I_{67} - 1 = 3.0(7)$ and $\alpha_2 = (I_{539} + I_{968})/I_{67} - 1 = 4.4(11)$, giving $\alpha = 3.4(6)$. BrICC calculations [39] yield $\alpha = 0.261$, 0.309, 3.71, and 4.69 for $E1$, $M1$, $E2$, and $M2$ radiation, respectively, favoring an $E2$ multipolarity. Thus, the 3005- and 3072-keV levels have same parity and differ most likely by $\Delta J = 2$. In this case, the Weisskopf estimate ratio of the isomeric half-life is $T_{1/2}/T_{1/2}^W \sim 3.5$. Its proximity to unity suggests that the 67-keV transition has single-particle character. Therefore, we used the Nilsson diagrams obtained by state-of-the-art Gogny HFB calculations [14] to identify possible 2-QP configurations corresponding to the identified
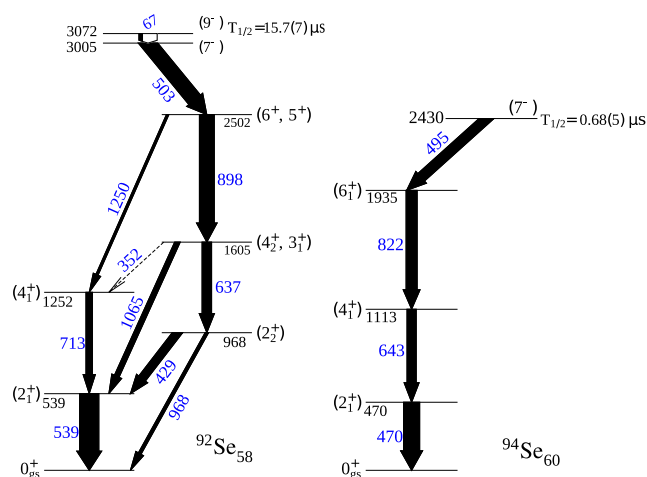

FIG. 2. Level schemes constructed for ^{92,94}Se. The arrow width of each transition indicates its intensity.
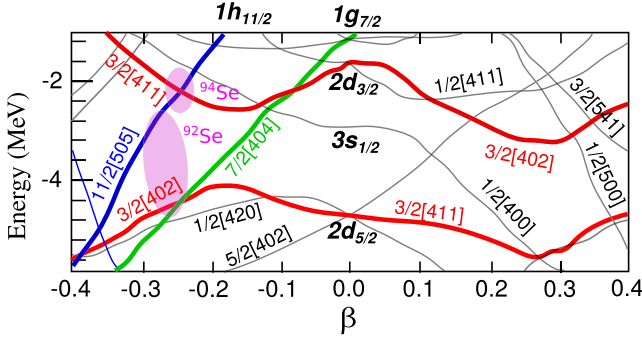
FIG. 3. Partial Nilsson diagrams for neutrons, obtained via Gogny Cranked HFB calculations for $Z = 34$, $N = 58$ [14]. Orbitals discussed in this Letter are highlighted with colored lines. Note that there is an avoided crossing of the two 3/2 orbitals around $\beta \sim -0.2$ where the orbitals exchange character. The configurations involved in the 2-QP states of $^{92}Se_{58}$ and $^{94}Se_{60}$ are highlighted by purple ellipsoids.

levels, see Fig. 3. A set of states coupling to 9^- and 7^- can only be identified for the two 2-QP neutron configurations $K^\pi = 7^-(\nu 11/2^-[505] \otimes \nu 3/2^+[402])$ and $K^\pi = 9^-(\nu 11/2^-[505] \otimes \nu 7/2^+[404])$, at oblate deformations of $\beta \sim -0.24$.

To complete the picture, we performed potential energy surface calculations using the configuration-constrained method of Xu *et al.* [40], with a Woods-Saxon potential and Lipkin-Nogami pairing. For each quasiparticle configuration, the occupied orbitals were fixed and the quadrupole, gamma, and hexadecapole deformation parameters $(\beta_2, \gamma, \beta_4)$ were varied in order to minimize the excitation energies. The neutron and proton monopole pairing strengths were determined by the average gap method [41]. Potential energy surfaces were calculated for the ground states and $K^\pi = 7^-(\nu 11/2^-[505] \otimes \nu 3/2^+[411])$, $K^\pi = 7^-(\nu 11/2^-[505] \otimes \nu 3/2^+[402])$, and $K^\pi = 9^-(\nu 11/2^-[505] \otimes \nu 7/2^+[404])$ configurations for $^{92,94}Se$. The results from these calculations for a selection of states are shown in Fig. 4, which show a structure that is consistent with the experimental observations. In particular, there is a large similarity in the deformations of the two configurations suggested for ^{92}Se, where the $K^\pi = 7^-(\nu 11/2^-[505] \otimes \nu 3/2^+[402])$ and $K^\pi = 9^-(\nu 11/2^-[505] \otimes \nu 7/2^+[404])$ configurations have $(\beta_2, \gamma, \beta_4) = (0.256, 52.9, 0.027)$ and $(\beta_2, \gamma, \beta_4) = (0.254, 54.1, 0.021)$, respectively. Thus, the transition between these configurations should only involve a single-particle orbital change from $\nu 7/2^+[404]$ to $\nu 3/2^+[402]$, supporting the single-particle interpretation of this state. The 7^- to 6^+ transition appears to be prompt within the experimental sensitivity. This is expected both from the K difference itself compared to ^{94}Se (see discussion below) and from the rather soft potential energy surface implying that K is a less well-defined quantum number in this 7^- configuration.

For ^{94}Se the isomeric decay was observed for the first time via γ rays within $0.19 \le t_\gamma \le 7.19$ μs [see Fig. 1(b)]. Similar to the procedure for ^{92}Se, a normalized background was subtracted from events within the time window $9 \le t_\gamma \le 23$ μs. In addition to the transitions reported in [10], new transitions with energies of 495, 752, 822, and 1180 keV were observed. Following the analysis steps as for ^{92}Se, a single isomeric state was found with $T_{1/2} = 0.68(5)$ μs. The transitions at 470.1(3), 642.6(3), 821.8(3), and 495.4(3) keV were observed all in mutual coincidence, decaying as a single cascade. Their placement in the level scheme shown in Fig. 2 was achieved through the comparison with the in-beam spectroscopy conducted simultaneously at F8, reporting two coincident transitions at 475(10) and 640(7) keV, plus a peaklike structure at 830(30) keV [10]. We also observed transitions at 751.5(4) and 1179.5(4) keV, however, with a lack of statistics for a $\gamma\gamma$-coincidence analysis. It is worth noting that these transitions could, in principle, originate from a parallel branch feeding the 470 keV transition and states above. This would require additional transitions associated with a decay pattern that is either too fragmented to be observed with the current statistics or of low enough energy to be below the efficiency threshold. The lifetime of the observed transitions is consistent with the other transitions in ^{94}Se, so the existence of a second isomer is unlikely, and the two γ rays at 752 and 1180 keV remain unplaced.
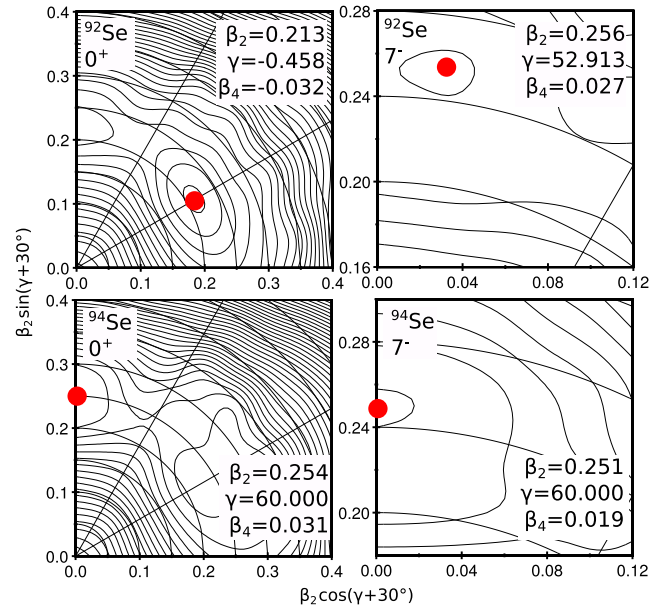

FIG. 4. Configuration-constrained potential energy surfaces for the ground states (left) and the 7^- states (right) of ^{92}Se (top) and ^{94}Se (bottom). The contours are separated by 100 keV and the potential energy surface minima are shown with a red dot. Note that the scales are different in the figures for the 7^- states. Also note that in these plots, β is always positive and oblate states correspond to $\gamma = 60$.

To interpret the isomeric state at 2430 keV, we evaluated the different potential J^π couplings along the Fermi surface that could match the decay scheme pattern. Only an oblate deformed ($\beta \sim -0.24$) 2-QP neutron state with configuration $K^\pi = 7^-(\nu 11/2^-[505] \otimes \nu 3/2^+[411])$ provides a consistent explanation as a K-forbidden decay. While the $K^\pi = 4^-$ coupling should be favorable in terms of level energy, the isomer is produced with high excitation energy and high angular momentum. The internal decay of these nuclei should primarily follow the yrast states and, thus, primarily reach the $K^\pi = 7^-$ bandhead, assuming similar moments of inertia as for the ground-state band. Recall that low-lying QP states are bandheads of rotational bands so their projection on the principal axis satisfies $|K^\pi| = J^\pi$. For the present case, an $E1$ $7^- \rightarrow 6^+$ transition leads to a forbiddenness $\nu = \Delta K - \lambda = 6$, a hindrance factor of $F_W = T_{1/2}/T_{1/2}^W = 2.49 \times 10^8$, and a reduced hindrance $f_\nu = F^{1/\nu} \sim 25$. Characteristic values for K traps are $F_W \gg 1$ and $f_\nu \sim 20$–300 [18], however, the $E1$ $\nu = 6$ decays known to date have a much more stringent distribution within $27 \lesssim f_\nu \lesssim 42$ [25,42].

The observed $J^\pi = 7^-$ states have very different decay paths for the two isotopes. In ^{92}Se, it decays almost exclusively to the $K = 2$ (yrare) band and not to the $K = 0$ (yrast) band. The different decay properties can be explained considering that the decay to the less K-forbidden branch is more likely, e.g., the $\nu = 4, 3$ decay to the $(6^+, 5^+)$ yrare level instead of the $\nu = 5$ to the 6^+ level of the ground-state band. In contrast, the 7^- state of ^{94}Se decays to the 6_1^+ level but not to any yrare level. This difference is unexpected, considering the rather smooth systematics of the yrare band beyond $N = 50$. Assuming the same smooth systematics, an extrapolation of the $(6^+, 5^+)$ state based on the 2_1^+ state to $N = 60$ leads to an expected excitation energy of this state in ^{94}Se around 2180 keV. This would give rise to a possible $\sim$250 keV transition to the yrare band, similar to what is observed in ^{92}Se. However, we did not observe such decay in this experiment so the yrare band is not within the energy ranges postulated, meaning a change of the structure at $N = 60$. For instance, the collective wave functions predicted by the SCCM method for ^{94}Se [10] propose a rigid oblate ground state and a rigid prolate yrare band, while both bands in ^{92}Se are γ soft.

In summary, this Letter presents the first observation and interpretation of an isomeric state of ^{94}Se in terms of a 2-QP neutron state with oblate deformation. Despite the rareness of such configurations in the nuclear chart, they provide experimental evidence of a property of the Nilsson levels: that oblate states can be formed for midshell nuclei whose Fermi surface reaches the Nilsson orbitals with high-j angular momentum sloping down. Moreover, the very different isomeric decay paths of each isotope are in sharp contrast with the rather smooth systematics of the ground-state and $K = 2$ excited bands of the selenium isotopic chain beyond the $N = 50$ shell closure. It not only suggests that a different and well-defined deformation exists for both bands but also indicates that the ground-state band of ^{94}Se has an oblate deformed shape, in line with the predictions of the SCCM calculations. Furthermore, with the existence of such isomers in this region, magnetic and electric moments could be measured in the future, keeping the oblate hypothesis open to verification by experiment.

[*]Corresponding author.
par.anders@eli-np.ro

[1] R. F. Casten, *Nuclear Structure from a Simple Perspective* (Oxford University Press, Oxford, 2000).

[2] W. Witt, V. Werner, N. Pietralla, M. Albers, A. D. Ayangeakaa, B. Bucher, M. P. Carpenter, D. Cline, H. M. David, A. Hayes *et al.*, Phys. Rev. C **98**, 041302(R) (2018).

[3] P. Singh, W. Korten, T. W. Hagen, A. Görgen, L. Grente, M.-D. Salsac, F. Farget, E. Clément, G. de France, T. Braunroth *et al.*, Phys. Rev. Lett. **121**, 192501 (2018).

[4] E. Cheifetz, R. C. Jared, S. G. Thompson, and J. B. Wilhelmy, Phys. Rev. Lett. **25**, 38 (1970).

[5] T. Togashi, Y. Tsunoda, T. Otsuka, and N. Shimizu, Phys. Rev. Lett. **117**, 172502 (2016).

[6] N. Gavrielov, A. Leviatan, and F. Iachello, Phys. Rev. C **99**, 064324 (2019).

[7] J. Litzinger, A. Blazhev, A. Dewald, F. Didierjean, G. Duchêne, C. Fransen, R. Lozeva, K. Sieja, D. Verney, G. de Angelis *et al.*, Phys. Rev. C **92**, 064322 (2015).

[8] T. Materna, W. Urban, K. Sieja, U. Köster, H. Faust, M. Czerwiński, T. Rząca-Urban, C. Bernards, C. Fransen, J. Jolie *et al.*, Phys. Rev. C **92**, 034305 (2015).

[9] I. N. Gratchev, G. S. Simpson, G. Thiamova, M. Ramdhane, K. Sieja, A. Blanc, M. Jentschel, U. Köster, P. Mutti, T. Soldner *et al.*, Phys. Rev. C **95**, 051302(R) (2017).

[10] S. Chen, P. Doornenbal, A. Obertelli, T. R. Rodríguez, G. Authelet, H. Baba, D. Calvet, F. Château, A. Corsi, A. Delbart *et al.*, Phys. Rev. C **95**, 041302 (2017).

[11] L. Wilets and M. Jean, Phys. Rev. **102**, 788 (1956).

[12] A. Davydov and G. Filippov, Nucl. Phys. **8**, 237 (1958).

[13] M. Lettmann, V. Werner, N. Pietralla, P. Doornenbal, A. Obertelli, T. R. Rodríguez, K. Sieja, G. Authelet, H. Baba, D. Calvet *et al.*, Phys. Rev. C **96**, 011301 (2017).

[14] J. P. Delaroche, M. Girod, J. Libert, H. Goutte, S. Hilaire, S. Péru, N. Pillet, and G. F. Bertsch, Phys. Rev. C **81**, 014303 (2010).

[15] T. R. Rodríguez, Phys. Rev. C **90**, 034306 (2014).

[16] K. Nomura, R. Rodríguez-Guzmán, and L. M. Robledo, Phys. Rev. C **95**, 064310 (2017).

[17] S. G. Nilsson, Mat. Fys. Medd. K. Dan. Vidensk. Selsk **29** (1955).

[18] P. M. Walker and F. R. Xu, Phys. Scr. **91**, 013010 (2016).

[19] P. Walker and G. Dracoulis, Nature (London) **399**, 35 (1999).

[20] G. D. Dracoulis, P. M. Walker, and F. G. Kondev, Rep. Prog. Phys. **79**, 076301 (2016).

[21] G. D. Dracoulis, Phys. Scr. **T88**, 54 (2000).

[22] M. Dasgupta, P. Walker, G. Dracoulis, A. Byrne, P. Regan, T. Kibédi, G. Lane, and K. Yeung, Phys. Lett. B **328**, 16 (1994).

[23] G. D. Dracoulis, G. J. Lane, A. P. Byrne, T. Kibédi, A. M. Baxter, A. O. Macchiavèlli, P. Fallon, and R. M. Clark, Phys. Rev. C **69**, 054318 (2004).

[24] G. D. Dracoulis, G. J. Lane, T. M. Peaty, A. P. Byrne, A. M. Baxter, P. M. Davidson, A. N. Wilson, T. Kibédi, and F. R. Xu, Phys. Rev. C **72**, 064319 (2005).

[25] F. Kondev, G. Dracoulis, and T. Kibédi, At. Data Nucl. Data Tables **103–104**, 50 (2015).

[26] T. Kubo, D. Kameda, H. Suzuki, N. Fukuda, H. Takeda, Y. Yanagisawa, M. Ohtake, K. Kusaka, K. Yoshida, N. Inabe *et al.*, Prog. Theor. Exp. Phys. **2012**, 03C003 (2012).

[27] A. Obertelli, A. Delbart, S. Anvar, L. Audirac, G. Authelet, H. Baba, B. Bruyneel, D. Calvet, F. Château, A. Corsi *et al.*, Eur. Phys. J. A **50**, 8 (2014).

[28] S. Takeuchi, T. Motobayashi, Y. Togano, M. Matsushita, N. Aoi, K. Demichi, H. Hasegawa, and H. Murakami, Nucl. Instrum. Methods Phys. Res., Sect. A **763**, 596 (2014).

[29] C. Santamaria, C. Louchart, A. Obertelli, V. Werner, P. Doornenbal, F. Nowacki, G. Authelet, H. Baba, D. Calvet, F. Château *et al.*, Phys. Rev. Lett. **115**, 192501 (2015).

[30] F. Flavigny, P. Doornenbal, A. Obertelli, J.-P. Delaroche, M. Girod, J. Libert, T. R. Rodriguez, G. Authelet, H. Baba, D. Calvet *et al.*, Phys. Rev. Lett. **118**, 242501 (2017).

[31] N. Paul, A. Corsi, A. Obertelli, P. Doornenbal, G. Authelet, H. Baba, B. Bally, M. Bender, D. Calvet, F. Château *et al.*, Phys. Rev. Lett. **118**, 032501 (2017).

[32] C. Shand, Z. Podolyák, M. Górska, P. Doornenbal, A. Obertelli, F. Nowacki, T. Otsuka, K. Sieja, J. Tostevin, Y. Tsunoda *et al.*, Phys. Lett. B **773**, 492 (2017).

[33] R. Taniuchi, C. Santamaria, P. Doornenbal, A. Obertelli, K. Yoneda, G. Authelet, H. Baba, D. Calvet, F. Château, A. Corsi *et al.*, Nature (London) **569**, 53 (2019).

[34] C. J. Griffin, T. Davinson, A. Estrade, D. Braga, I. Burrows, P. Coleman-Smith, T. Grahn, A. Grant, L. J. Harkness-Brennan, M. Kogimtzis *et al.*, Proc. Sci., NICXIII2014 (**2014**) 097.

[35] P.-A. Söderström, S. Nishimura, P. Doornenbal, G. Lorusso, T. Sumikama, H. Watanabe, Z. Y. Xu, H. Baba, F. Browne, S. Go *et al.*, Nucl. Instrum. Methods Phys. Res., Sect. B **317**, 649 (2013).

[36] D. Kameda, T. Kubo, T. Ohnishi, K. Kusaka, A. Yoshida, K. Yoshida, M. Ohtake, N. Fukuda, H. Takeda, K. Tanaka *et al.*, Phys. Rev. C **86**, 054319 (2012).

[37] R.-B. Gerst, A. Blazhev, N. Warr, J. N. Wilson, M. Lebois, N. Jovančević, D. Thisse, R. Canavan, M. Rudigier, D. Étasse *et al.* (to be published).

[38] C. Lizarazo, Gamma-ray spectroscopy of ^{92,94}Se isomeric decay, Ph.D. thesis, Technische Universität Darmstadt, 2018.

[39] T. Kibédi, T. Burrows, M. Trzhaskovskaya, P. Davidson, and C. N. Jr., Nucl. Instrum. Methods Phys. Res., Sect. A **589**, 202 (2008).

[40] F. R. Xu, P. M. Walker, J. A. Sheikh, and R. Wyss, Phys. Lett. B **435**, 257 (1998).

[41] P. Moller and J. R. Nix, Nucl. Phys. **A536**, 20 (1992).

[42] Z. Patel, P. M. Walker, Z. Podolyák, P. H. Regan, T. A. Berry, P.-A. Söderström, H. Watanabe, E. Ideguchi, G. S. Simpson, S. Nishimura *et al.*, Phys. Rev. C **96**, 034305 (2017).